THE JOURNAL OF PHYSICAL CHEMISTRY Letters

Letter

pubs.acs.org/JPCL

Electron–Phonon Coupling Strength at Metal Surfaces Directly Determined from the Helium Atom Scattering Debye–Waller Factor

J. R. Manson,*[,†,‡] G. Benedek,[‡,§] and Salvador Miret-Artés[‡,∥]

[†]Department of Physics and Astronomy, Clemson University, Clemson, South Carolina 29634, United States

[‡]Donostia International Physics Center (DIPC), Paseo Manuel de Lardizabal, 4 20018 Donostia-San Sebastian, Spain

[§]Dipartimento di Scienza dei Materiali, Università di Milano-Bicocca, Via Cozzi 53, 20125 Milano, Italy

[∥]Instituto de Física Fundamental, Consejo Superior de Investigaciones Científicas, Serrano 123, 28006 Madrid, Spain

ABSTRACT: A new quantum-theoretical derivation of the elastic and inelastic scattering probability of He atoms from a metal surface, where the energy and momentum exchange with the phonon gas can occur only through the mediation of the surface free-electron density, shows that the Debye–Waller exponent is directly proportional to the electron–phonon mass coupling constant λ. The comparison between the values of λ extracted from existing data on the Debye–Waller factor for various metal surfaces and the λ values known from literature indicates a substantial agreement, which opens the possibility of directly extracting the electron–phonon coupling strength in quasi-2D conducting systems from the temperature or incident energy dependence of the elastic helium atom scattering intensities.

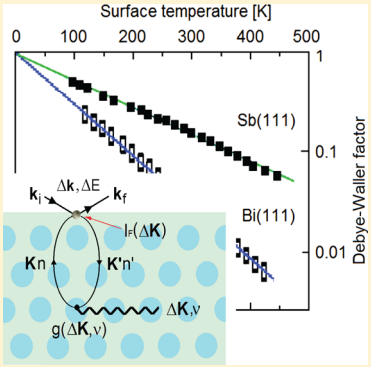

An atom at thermal energy scattered by a metal surface can exchange energy with the phonon gas of the solid through oscillations of the electron density produced at the surface by the vibrational displacements of the atomic cores. Thus, the inelastic atom scattering intensity when a phonon is created or annihilated has been shown to be approximately proportional to the electron–phonon (e-p) coupling constant (mass correction factor) $\lambda_{\mathbf{Q},\nu}$ for that specific phonon mode of branch index ν and parallel wavevector $\mathbf{Q}$. This was recently demonstrated for ultrathin lead films[1,2] and the Bi(111) surface,[3] enabling the so-called *mode–λ* spectroscopy for the determination of individual phonon contributions to the mass correction factor. The average of the coupling strength over the phonon spectrum defines the coupling constant λ as $\lambda = \langle\lambda_{\mathbf{Q},\nu}\rangle$.[4,5]

We show that the application of standard approximations of electron–phonon coupling theory for metals to the distorted wave Born approximation (DWBA) for atom-surface scattering leads to expressions that relate the elastic and inelastic scattering intensities as well as the Debye–Waller (DW) factor to the mass correction factor of superconductivity theory. This treatment, besides reproducing the previous result that the intensities for single-phonon inelastic peaks in the scattered spectra are proportional to the respective phonon mode components $\lambda_{\mathbf{Q},\nu}$, leads to a new and useful formulation for the Debye–Waller factor $\exp\{-2W(T_S)\}$. Because the intensities of elastic diffraction peaks are proportional to the Debye–Waller factor, their logarithmic temperature dependence at sufficiently large absolute temperature T_S is a linear function of T_S with a slope approximately proportional to the coupling constant λ. Not only does this work demonstrate that λ and its mode components can be measured in molecule–surface collision experiments, but also it shows how phonon-induced modulation to the molecule–surface interaction potential is related to the surface electron coupling strength at the surface of metals. Knowledge of the interaction potential is important for understanding adsorption, chemisorption, or chemical reactions on metal surfaces.[6,7]

In the distorted wave formalism employed here, the important static parts of the potential such as the van der Waals attraction with its associated adsorption well and also the overall repulsive part are contained in the distorted wave functions of the scattering atom. The colliding He atom is repelled by the surface electron density $n(\mathbf{r})$. In the absence of lattice vibrations $n(\mathbf{r}) = \sum_{\mathbf{K},n}|\psi_{\mathbf{K},n}(\mathbf{r})|^2$, where $\psi_{\mathbf{K},n}(\mathbf{r}) = \exp\{i\mathbf{K}\cdot R\}\varphi_{\mathbf{K},n}(z)$ are the electron wave functions of the occupied states that contribute to the surface density at the comparatively large distance (~3 Å) from the first surface atomic plane where He atoms are repelled (classical turning point). In practice $n(\mathbf{r})$ receives the largest contribution from free electrons at the Fermi level, which allows for the factorization of wave functions into a simple plane wave of parallel wave vector $\mathbf{K}$ and band index n and the wave function $\varphi_{\mathbf{K},n}(z)$ for the motion normal to the surface, with $\mathbf{r} = (\mathbf{R}, z)$. Summations over $\{\mathbf{K}, n\}$ implicitly include a factor of 2 for spin. Multiplying this electron density by the Ebsjerg–Nørskov constant A_N gives the repulsive part of the distorting potential extending outside of the terminal

Received: January 21, 2016
Accepted: February 29, 2016
Published: February 29, 2016

DOI: 10.1021/acs.jpclett.6b00139
J. Phys. Chem. Lett. 2016, 7, 1016–1021

surface layer of core atoms.[8−10] The interaction potential $\mathcal{V}(\mathbf{r})$, which is regarded as a perturbation on the distorting potential, is then proportional to the variation in the electronic density caused by electron−phonon coupling

$$\mathcal{V}(\mathbf{r}) = A_N \delta n(\mathbf{r}) = A_N \sum_{\mathbf{K},n} \{|\tilde{\psi}_{\mathbf{K},n}|^2 - |\psi_{\mathbf{K},n}|^2\} \tag{1}$$

where $\tilde{\psi}_{\mathbf{K},n}$ is the wave function with electron−phonon coupling to the cores and is related to $\psi_{\mathbf{K},n}$ through ordinary second-order perturbation theory via the electron matrix elements

$$\tilde{\psi}_{\mathbf{K},n} = \psi_{\mathbf{K},n} + \sum_{\mathbf{K}',n'}{}' \psi_{\mathbf{K}',n'} \frac{(\psi_{\mathbf{K}',n'}|V^{\mathrm{el}}|\psi_{\mathbf{K},n})}{E^{\mathrm{el}}_{\mathbf{K},n} - E^{\mathrm{el}}_{\mathbf{K}',n'}} \tag{2}$$

where the prime symbol indicates that the state $\{\mathbf{K}, n\}$ is excluded from the sum.

The electron−phonon interaction comes about through the electronic potential V^{el} written as a sum over the pairwise pseudopotentials $v^{\mathrm{el}}(\mathbf{r} - \mathbf{r}_l - \mathbf{u}_l(t))$ between the electron at position $\mathbf{r}$ and the ions at the instantaneous positions $\mathbf{r}_l + \mathbf{u}_l(t)$, with $\mathbf{u}_l(t)$ being their vibrational displacements and l being a 3D integer index labeling the lattice sites.

In the following we shall use formal scattering theory with initial (i) and final (f) distorted states $\exp\{i\mathbf{K}_{i,f}\cdot\mathbf{R}\}\,\chi_{k_{iz},k_{fz}}(z)\,|n_{i,f}\rangle$ of the He surface system, where $\chi_{k_{iz},k_{fz}}(z)$ are the He atom initial and final distorted states for motion normal to the surface and $|n_{i,f}\rangle$ are the many-body phonon states of the target crystal before and after scattering. The transition rate for purely elastic diffraction is found to be

$$w^{(0)}_{\mathrm{DWBA}}(\mathbf{k}_f, \mathbf{k}_i) = \frac{8\pi A_N^2}{\hbar a_c^2} \sum_{\mathbf{G}} e^{-2W^{\mathrm{eff}}(\mathbf{k}_f,\mathbf{k}_i)} \sum_{\mathbf{K},n} \left| \Re \sum_{n'}{}' \frac{(\chi_{k_{iz}}(z)|\varphi^*_{\mathbf{K},n}(z)\varphi_{\mathbf{K}+\mathbf{G},n'}(z)|\chi_{k_{fz}}(z))}{E^{\mathrm{el}}_{\mathbf{K},n} - E^{\mathrm{el}}_{\mathbf{K}+\mathbf{G},n'}} \times \sum_j (\varphi_{\mathbf{K}+\mathbf{G},n'}(z)|v^{\mathrm{el,eff}}_{\mathbf{G}}(T_S, z - z_j)|\varphi_{\mathbf{K},n}(z)) \right|^2 \times \delta_{\mathbf{K}_f - \mathbf{K}_i, \mathbf{G}}\, \delta(E_f - E_i) \tag{3}$$

where $\Re$ signifies the real part, j is an index labeling the planes parallel to the surface, and a_c is the area of the unit cell.

As shown in eq 3, the overlap integral matrix element $(\chi_{k_{iz}}(z)|\varphi^*_{\mathbf{K},n}(z)\varphi_{\mathbf{K}+\Delta\mathbf{K},n'}(z)|\chi_{k_{fz}}(z)) \equiv I_F(\Delta\mathbf{K})$ is taken over a nondiagonal element of the electron density operator, which acts as the effective scattering potential of the He-atom distorted waves. Contributions to this overlap integral come almost entirely from electrons near the Fermi energy, as indicated by the subscript F. Outside the surface and in front of the terminating layer of cores the electron wave functions decrease roughly exponentially with a decay constant dictated by the work function. The projectile wave functions are even more strongly decaying in the opposite direction into the surface electron density. The overlap between these two opposing behaviors defines the thin 2-D surface region where the interaction takes place, and this essentially contains the locus of classical turning points. Equation 3 is associated with an effective temperature-dependent Debye−Waller factor $\exp\{-2W^{\mathrm{eff}}(\mathbf{k}_f, \mathbf{k}_i)\}$ which accounts for the modulation of the surface charge density induced by the ion thermal fluctuations. The remaining matrix element accounts for the scattering of the virtual electron from the lattice ion potential mediated on the thermal oscillations. Thus, also the ion pseudopotential is mediated on thermal ion fluctuations at the surface temperature T_S, and its 2D Fourier component is indicated in eq 3 as $v^{\mathrm{el,eff}}_{\Delta\mathbf{K}}(T_S, z - z_j)$. Equation 3 shows that the electron−phonon interaction induces a static corrugation in the electronic density that produces diffraction peaks when the parallel momentum transfer $\Delta\mathbf{K} = \mathbf{K}_f - \mathbf{K}_i$ is a surface reciprocal lattice vector $\mathbf{G}$.

The one-phonon transition rate allows us to identify the effective Debye−Waller factor $\exp\{-2W^{\mathrm{eff}}(\mathbf{k}_f, \mathbf{k}_i)\}$ that appears as a multiplicative factor in all scattered intensities, and its argument is given by

$$2W^{\mathrm{eff}}(\mathbf{k}_f, \mathbf{k}_i) = 4 \sum_{\mathbf{Q},\nu} \frac{\hbar}{NM\omega_{\mathbf{Q},\nu}} \sum_{\mathbf{K},n} \times \left| \sum_{\alpha=1}^{3} \Delta k_\alpha P_\alpha(T_S; \mathbf{Q}, \mathbf{K}, \nu, n) \right|^2 \left[n_{\mathrm{BE}}(\omega_{\mathbf{Q},\nu}) + \frac{1}{2} \right] \tag{4}$$

where $\hbar\Delta k_\alpha = \hbar(\mathbf{k}_f - \mathbf{k}_i)_\alpha$ are Cartesian components of the momentum transfer vector and N is the number of atoms. The electron−phonon coupling, which relates the mean square displacement of the electron density at the point of impact to that of the atomic cores, is contained in the factors of

$$P_\alpha(T_S; \mathbf{Q}, \mathbf{K}, \nu, n) = \Re \sum_j \sum_{n'}{}' \frac{I_F(\Delta\mathbf{K}) e_\alpha(\mathbf{Q}, \nu)}{(\chi_{k_{iz}}(z)|\hat{q}_\alpha n^{\mathrm{eff}}_{\mathbf{Q}}(T_S, z)|\chi_{k_{fz}}(z))} \times \frac{(\varphi^*_{\mathbf{K}-\mathbf{Q},n'}(z)|\hat{q}_\alpha v^{\mathrm{el,eff}}_{\mathbf{Q}}(T_S, z - z_j)|\varphi_{\mathbf{K},n}(z))}{E^{\mathrm{el}}_{\mathbf{K},n} - E^{\mathrm{el}}_{\mathbf{K}-\mathbf{Q},n'}} \tag{5}$$

where $\hat{q}_\alpha$ is a Cartesian component of the vector operator $\hat{\mathbf{q}} = \{\mathbf{Q}, id/dz\}$ and $e_\alpha(\mathbf{Q}, \nu)$ is a component of the phonon polarization vector. The matrix element of the repulsive potential is $(\chi_{k_{fz}}(z)|\hat{q}_\alpha n^{\mathrm{eff}}_{\mathbf{Q}}(T_S, z)|\chi_{k_{iz}}(z))$, and it receives its contribution entirely from the narrow region of the classical turning points.

It is noteworthy that the Ebsjerg-Nørskov constant A_N does not appear in the D-W factor. This is an important observation because it means that the effective Debye−Waller factor is based only on the very general principle that the part of the atom-surface potential that gives rise to energy transfer is proportional to the surface electron density, but does not depend on the actual value of the proportionality constant.

Notable also is the fact that the dependence on initial and final projectile momenta is substantially more complex than the simple quadratic dependence on $\Delta\mathbf{k} = \mathbf{k}_f - \mathbf{k}_i$ encountered in standard DW treatments, e.g., as in neutron scattering. This more complex momentum dependence, as well as the dependence on the attractive adsorption well in the interaction potential, is introduced through the presence of the distorted atomic wave functions. The polarization vectors as well as the mass M in eqs 4 and (5) are those of the crystal cores. It is the electron−phonon coupling, via the e-p matrix elements, that produces the actual effective vibrational mean-square displacement vectors experienced by the colliding projectile interacting with the electron gas in front of the surface. As an added comment, the Debye−Waller exponent contains additional

DOI: 10.1021/acs.jpclett.6b00139
J. Phys. Chem. Lett. 2016, 7, 1016−1021

dependence on the temperature over and above that of the Bose–Einstein functions appearing explicitly. This additional temperature dependence is contained in the effective potentials $n_{\mathbf{Q}}^{\mathrm{eff}}(T_S,z)$ and $v_{\mathbf{Q}}^{\mathrm{el,eff}}(T_S, z - z_j)$ appearing in eq 5 and arises directly from the electron contribution to the Debye–Waller factor.

Rather than continuing with complete results, which are discussed in detail elsewhere,[11] it is of interest to apply approximations valid for metals and to exhibit the inelastic intensity and Debye–Waller factor in terms of the standard definitions of the e-p coupling constant. The restriction to the Fermi level allows the standard Grimvall approximation (especially appropriate for single phonon transitions) $E_{\mathbf{K},n}^{\mathrm{el}} - E_{\mathbf{K}-\Delta\mathbf{K},n'}^{\mathrm{el}} = \hbar\omega_{\Delta\mathbf{K},\nu}$, where $\hbar\omega_{\Delta\mathbf{K},\nu}$ is the phonon energy.[5] The electron–phonon coupling matrix is usually written with the following definition[1,4,5,12]

$$g_{n,n'}(\mathbf{K},\Delta\mathbf{K},\nu) \equiv \sum_j \left[\frac{\hbar}{2NM\omega_{\Delta\mathbf{K},\nu}}\right]^{1/2} \mathbf{e}(\Delta\mathbf{K},\nu) \cdot(\varphi^*_{\mathbf{K}-\Delta\mathbf{K},n'}(z)|\hat{q}v^{\mathrm{el,eff}}_{\Delta\mathbf{K}}(T_S, z - z_j)|\varphi_{\mathbf{K},n}(z)) \tag{6}$$

and the mode-specific components of λ are[4]

$$\lambda_{\mathbf{Q},\nu} = \frac{2}{\mathcal{N}(E_F)[\hbar\omega_{\mathbf{Q},\nu}]^3}\sum_{\mathbf{K},n}\left|\sum_{n'} g_{n,n'}(\mathbf{K},\mathbf{Q},\nu)\right|^2 \tag{7}$$

where the summation over electron wave vectors involves only states near the Fermi surface and $\mathcal{N}(E_F)$ is the density of electron states at the Fermi surface. The definition for $g_{n,n'}(\mathbf{K},\Delta\mathbf{K},\nu)$, and hence that for $\lambda_{\mathbf{Q},\nu}$, differs slightly from the standard definitions[4,5] in that an effective, temperature-dependent electron–phonon potential now appears in the matrix element in our treatment. This arises from the electronic Debye–Waller considerations that we have introduced into this treatment.

The inelastic He-atom scattering (HAS) process is illustrated by the diagram of Figure 1, in which an incident projectile atom

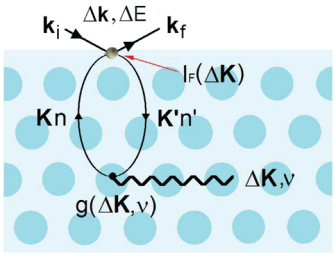

Figure 1. An incident atom in a state of wavevector $\mathbf{k}_i$ is inelastically scattered into a final state of wavevector $\mathbf{k}_f$ by the overlap vertex $I_F(\Delta\mathbf{K})$ and creates a phonon of wavevector $\Delta\mathbf{K}$ and branch index ν via a virtual electron–hole pair of states and the electron–phonon vertex term g.

in a state of wavevector $\mathbf{k}_i$ is inelastically scattered into a final state of wavevector $\mathbf{k}_f$, eventually creating a phonon of wavevector $\Delta\mathbf{K}$ and branch index ν via the mediation of a virtual electron–hole pair involving the electronic states at the Fermi level of parallel wavevectors $\mathbf{K}$ and $\mathbf{K}'$ and band indices n and n'. The nondiagonal electron density matrix element $I_F(\Delta\mathbf{K})$ acts as an effective scattering potential, whose matrix element between the initial and final atom states provides the upper vertex term, whereas the lower vertex term is expressed by the electron–phonon matrix element $g_{n,n'}(\mathbf{K},\Delta\mathbf{K},\nu)$. It is important to remark that the phonon can be generated near the surface or, as depicted in Figure 1, at several atomic planes beneath the surface, with the maximum depth being determined by the range of the e-p interaction (quantum sonar effect).[1,2,11]

Combining the above e-p approximations and definitions casts the single phonon inelastic transition rate into the form

$$w^{(1)}_{\mathrm{DWBA}}(\mathbf{k}_f,\mathbf{k}_i) = \frac{4\pi A_N^2}{\hbar a_c^2}\mathcal{N}(E_F)e^{-2W^{\mathrm{eff}}(\mathbf{k}_f,\mathbf{k}_i)} \times \sum_\nu \hbar\omega_{\Delta\mathbf{K},\nu}|I_F(\Delta\mathbf{K})|^2\lambda_{\Delta\mathbf{K},\nu} \times |n_{BE}(\omega_{\Delta\mathbf{K},\nu})|\delta(E_f - E_i - \hbar\omega_{\Delta\mathbf{K},\nu}) \tag{8}$$

This is similar to the new result of Sklyadneva et al.[1,2] showing that the probability of creating (or annihilating) a phonon mode $\{\mathbf{Q},\nu\}$ with frequency $\omega_{\mathbf{Q},\nu}$ is proportional to the respective mode-dependent electron–phonon coupling constant $\lambda_{\mathbf{Q},\nu}$; however, eq 8 contains an effective DW factor, an important difference with respect to the previous work,[1,2] where the one-phonon approximation was made before the thermal average over the phonon ensemble, and no DW factor is found in that case.

It is of interest to examine the Debye–Waller exponent $2W^{\mathrm{eff}}$ under reasonable approximations applicable to elastic diffraction. Because the Debye–Waller argument is expressed as a sum over all contributing phonon modes for a given set of experimental initial incident beam and final detector parameters, it will of necessity be expressed as a weighted summation over the mode-specific $\lambda_{\mathbf{Q},\nu}$. The simplest case, and the configuration that is most often measured, is the specular diffraction peak in which the parallel momentum exchange vanishes and the total momentum transfer is $2k_{iz}$ entirely in the direction normal to the surface. In this case, considering an exponential decay $\exp\{-2\kappa z\}$ for the electron density at the He-atom turning point, with $\kappa = \sqrt{2m_e^*\phi}/\hbar$, where ϕ is the work function and m_e^* is the electron effective mass, leads to

$$2W^{\mathrm{eff}}(\mathbf{k}_f,\mathbf{k}_i) = \frac{\mathcal{N}(E_F)}{3N}\frac{m}{m_e^*}\frac{E_{iz}}{\phi}\sum_{\mathbf{Q},\nu}\hbar\omega_{\mathbf{Q},\nu}\lambda_{\mathbf{Q},\nu} \times \left|\frac{I_F(\mathbf{Q})}{(\chi_{k_{iz}}(z)|n_{\mathbf{Q}}^{\mathrm{eff}}(T_S,z)|\chi_{k_{fz}}(z))}\right|^2\left[n_{BE}(\omega_{\mathbf{Q},\nu}) + \frac{1}{2}\right] \tag{9}$$

where m is the He atom mass and $E_{iz} = \hbar^2k_{iz}^2/2m$ is the normal part of the He atom incident energy. Equation 9 shows the Debye–Waller exponent expressed explicitly as a weighted summation over $\lambda_{\mathbf{Q},\nu}$. The weighting coefficients are quantities that can be readily evaluated, that is, the squared ratio of the overlap integral and the distorted wave matrix elements of the repulsive potential, and in many cases this ratio is nearly unity, for example, in the case of weakly corrugated metals. Thus, in the high-temperature limit where $n_{BE} \to k_BT_S/\hbar\omega_{\mathbf{Q},\nu}$, the Debye–Waller exponent for specular diffraction is proportional to λ

$$2W^{\mathrm{eff}}(\mathbf{k}_f,\mathbf{k}_i) \cong \mathcal{N}(E_F)\frac{m}{m_e^*}\frac{E_{iz}}{\phi}\lambda k_BT_S \tag{10}$$

DOI: 10.1021/acs.jpclett.6b00139
J. Phys. Chem. Lett. 2016, 7, 1016–1021

Thus, the coupling constant λ can be directly obtained from the temperature dependence of the HAS specular intensity I_{00} as

$$\lambda_{HAS} \cong -\frac{1}{\mathcal{N}(E_F)} \frac{d \ln I_{00}}{k_B d T_S} \frac{m_e^*}{m} \frac{\phi}{E_{iz}} \quad (11)$$

provided the electronic density of states and effective mass at the Fermi level are known. In general, the tail of the electron density far away from the surface atomic plane, where the He atoms are reflected, receives a major contribution from the surface states at the Fermi level. For a simple estimation, the free electron expression $m_e^*/\mathcal{N}(E_F) = \hbar^2 k_F^2/3Z$ may be used, where k_F is the Fermi wavevector and Z is the number of free electrons per atom.

As an example, we show in Figure 2 recent measurements of the logarithmic thermal attenuation (DW plots) of the HAS specular intensity from the Sb(111)[13] and Bi(111)[14] surfaces. The corresponding values of λ_{HAS} extracted from eq 11 under the free-electron assumption are 0.28 and 0.57, respectively, and compare favorably with the surface values reported by Hofmann for Bi(111)[17] and calculated ab initio by Campi et al. for Sb(111).[29] A list of these and other values for a selection of metal surfaces appears in Table 1, and the agreements between the surface and known bulk values of λ are quite reasonable.

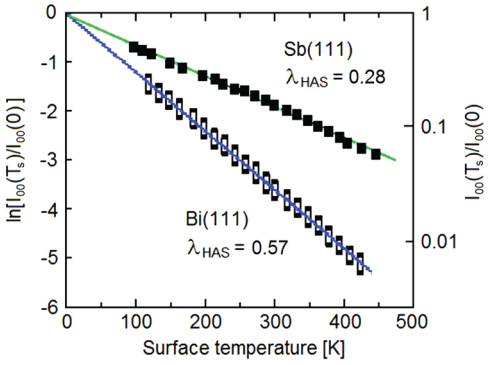

Figure 2. Debye–Waller plots of the specular intensity versus T_S for He atom scattering from Sb(111) and Bi(111). Data for Sb(111) from ref 13 and for Bi(111) from ref 14.

Some comments about the data presented in Table 1 are in order. The experimental HAS data for Pb(111) taken from refs 24 and 26 are for the specific case of seven monolayers of Pb on a Cu(111) substrate. It is also evident from the list of measured values of λ from other sources, particularly for the cases of Bi(111) and Cu(110), that there can be significant variations in reported values. Finally, a value of λ = 1.3 for Bi(111) has recently been reported.[3] This value, which was obtained by comparing energy-resolved inelastic HAS scattering spectra for Bi(111) with those of Pb(111), is larger than that reported here obtained from Debye–Waller factor measurements on the specular diffraction peak and also larger than the values reported from other sources; however, inelastic HAS spectra sample only a limited number of phonon modes, namely, only those modes that can be accessed along the He atom scan curve. The scan curve, which results from energy and momentum conservation parallel to the surface, appears in a plot of energy transfer versus $\Delta\mathbf{K}$ as a parabolic function, whose shape is determined by the incident He atom beam energy and angles and the angular position of the detector. Only those phonons with both energy $\hbar\omega_{\Delta K,\nu}$ and parallel momentum $\Delta\mathbf{K}$ lying on the scan curve are accessible in an inelastic HAS spectrum for a given set of experimental conditions. When, as a trial estimate of λ, the average over $\{\mathbf{Q}, \nu\}$ is restricted to a selected set of phonons, for example, those sampled by HAS along a single scan curve, trial values of λ dispersed over a fairly large range may be found. This is illustrated by the interesting example of Bi(111) versus Pb(111) in ref 3, where a ratio of $\lambda_{Pb}/\lambda_{Bi}$ = 1.35 was obtained from similar HAS scan curves for each of the two metals. This is in contrast with the ratio of 0.75, a factor of ~2 smaller, from the Debye–Waller factors reported in Table 1, and means that under the kinematic conditions of ref 3 the phonons sampled in Bi(111) make a larger contribution to e-p interaction than in the 7 ML-Pb(111) film. The comparison is interesting because Pb is a bulk superconductor with transition temperature decreasing from bulk to ultrathin films, whereas bulk Bi is not a superconductor, but it becomes so in reduced dimensionality,[36] possibly because of some specific surface-localized phonons with particularly strong e-p coupling. Thus, sampling different segments of the phonon spectrum with inelastic HAS may help in pinpointing which phonons are actually important for electron pairing in low-dimensional superconductors. The Debye–Waller factor, on the contrary, is not similarly limited by the scan curve and hence is able to produce the true and correctly averaged λ for a given surface.

This treatment, based on electron–phonon interaction theory, determines the corrugation and vibrational displacements of the electron gas in front of a surface at the locus of points where an incoming atom is reflected. All aspects of the scattering are related to the electron–phonon coupling constants. The single-phonon scattered intensity shows that the vibrational displacements of the electron density above the

Table 1. Mass Enhancement Factor λ_{HAS} Expressing the Electron–Phonon Interaction As Derived from the Temperature Dependence of the HAS Specular Intensity (eq 11 with the free-electron assumption) for Selected Conducting Surfaces and Compared with Values of λ from Other Sources As Cited[a]

surface	Bi(111)	Cu(110)	Pb(111)	Sb(111)	W(001)1X1
$-d \ln I_{00}/dT_S$ ($10^{-3}K^{-1}$)	11.5[14]	1.7[18]	5.0[24]	5.6[13]	4.1[30]
k_{iz}^2 (Å^{-2})	16.79[14]	6.20[18]	5.65[24,26]	22.8[13]	26.3[30]
ϕ (eV)	4.23[15]	4.48[19]	4.25[25]	4.56[27]	4.32[31]
k_F (Å^{-1})	0.72[16]	0.25[20]	0.65[2]	0.80[28]	1.09[32]
λ_{HAS}	0.57	0.15	0.76	0.28	0.31
λ (other sources)	0.60[17]	0.17[21]	0.95[2]	0.27[29]	0.28[33]
	0.45[35]	0.23[22,23]	0.7–0.9[34]		

[a]In the column marked Pb(111), the experimental data from ref 24 and the value given for λ_{HAS} are for seven monolayers of Pb on a Cu(111) substrate.

DOI: 10.1021/acs.jpclett.6b00139
J. Phys. Chem. Lett. 2016, 7, 1016–1021

surface may be quite different from those of the core atoms, and even the polarizations for the same phonon mode may be in different directions; however, the displacements of the electron density are expressed directly in terms of the masses and polarization vectors of the crystal cores. Of particular importance, the single phonon scattering intensities are proportional to the mode-specific electron−phonon constants $\lambda_{Q,\nu}$, and the argument of the Debye−Waller factor is to a good approximation proportional to the electron−phonon coupling constant λ.

AUTHOR INFORMATION

Corresponding Author

*E-mail: jmanson@clemson.edu.

Notes

The authors declare no competing financial interest.

ACKNOWLEDGMENTS

G.B. thanks Prof. Marco Bernasconi for helpful discussions. This work is partially supported by a grant with ref. FIS2014-52172-C2-1-P from the Ministerio de Economia y Competitividad (Spain).

REFERENCES

(1) Sklyadneva, I. Yu.; Benedek, G.; Chulkov, E. V.; Echenique, P. M.; Heid, R.; Bohnen, K.-P.; Toennies, J. P. Mode-Selected Electron-Phonon Coupling in Superconducting Pb Nanofilms Determined from He Atom Scattering. *Phys. Rev. Lett.* **2011**, *107*, 095502.

(2) Benedek, G.; Bernasconi, M.; Bohnen, K.-P.; Campi, D.; Chulkov, E. V.; Echenique, P. M.; Heid, R.; Sklyadneva, I. Yu.; Toennies, J. P. Unveiling mode-selected electron-phonon interactions in metal films by helium atom scattering. *Phys. Chem. Chem. Phys.* **2014**, *16*, 7159−7172.

(3) Tamtögl, A.; Kraus, P.; Mayrhofer-Reinhartshuber, M.; Campi, D.; Bernasconi, M.; Benedek, G.; Ernst, W. E. Surface and subsurface phonons of Bi(111) measured with helium atom scattering. *Phys. Rev. B: Condens. Matter Mater. Phys.* **2013**, *87*, 035410.

(4) Allen, P. B. Neutron spectroscopy of superconductors. *Phys. Rev. B* **1972**, *6*, 2577−2579.

(5) Grimvall, G. *The Electron-Phonon Interaction in Metals*; North-Holland: New York, 1981; Chapter 4.

(6) For a perspective and extensive references see: Kroes, G.-J. Toward a Database of Chemically Accurate Barrier Heights for Reactions of Molecules with Metal Surfaces. *J. Phys. Chem. Lett.* **2015**, *6*, 4106−4114.

(7) Bünermann, O.; Jiang, H.; Dorenkamp, Y.; Kandratsenka, A.; Janke, S. M.; Auerbach, D. J.; Wodtke, A. M. Electron-hole pair excitation determines the mechanism of hydrogen atom adsorption. *Science* **2015**, *350*, 1346−1349.

(8) Esbjerg, N.; Nørskov, J. K. Dependence of the He-scattering potential at surfaces on the surface-electron-density profile. *Phys. Rev. Lett.* **1980**, *45*, 807−810.

(9) Senet, P.; Toennies, J. P.; Benedek, G. Theory of the He-phonon forces at a metal surface. *Europhys. Lett.* **2002**, *57*, 430−436.

(10) Chizmeshya, A.; Zaremba, E. The interaction of rare-gas atoms with metal-surfaces - a scattering-theory approach. *Surf. Sci.* **1992**, *268*, 432−456.

(11) Manson, J. R.; Benedek, G.; Miret-Artés, S., unpublished.

(12) (a) Eliashberg, G. M. *Zh. Eksp. Teor. Fiz.* **1960**, *38*, 966;(b) Interactions between electrons and lattice vibrations in a superconductor. *Soviet Phys. - JETP* **1960**, *11*, 696−702. (c) Eliashberg, G. M. *Zh. Eksp. Teor. Fiz.* **1962**, *43*, 1005;(d) The Low Temperature Specific Heat of Metals. *Soviet Phys. - JETP* **1963**, *16*, 780−781.

(13) Tamtögl, A.; Mayrhofer-Reinhartshuber, M.; Kraus, P.; Ernst, W. E. Surface Debye temperature and vibrational dynamics of Antimony(111) from helium atom scattering measurements. *Surf. Sci.* **2013**, *617*, 225−228.

(14) Mayrhofer-Reinhartshuber, M.; Tamtögl, A.; Kraus, P.; Rieder, K. H.; Ernst, W. E. Vibrational dynamics and surface structure of Bi(111) from helium atom scattering measurements. *J. Phys.: Condens. Matter* **2012**, *24*, 104008.

(15) Bronner, Ch.; Tegeder, P. Unoccupied electronic band structure of the semi-metallic Bi(111) surface probed with two-photon photoemission. *Phys. Rev. B: Condens. Matter Mater. Phys.* **2013**, *87*, 035123.

(16) Ohtsubo, Y.; Perfetti, L.; Goerbig, M. O.; Le Fèvre, P.; Bertran, F.; Taleb-Ibrahimi, A. Non-trivial surface-band dispersion on Bi(111). *New J. Phys.* **2013**, *15*, 033041.

(17) Hofmann, P. The surfaces of bismuth: Structural and electronic properties. *Prog. Surf. Sci.* **2006**, *81*, 191−245.

(18) Lapujoulade, J.; Perreau, J.; Kara, A. The thermal attenuation of elastic-scattering of helium from copper single-crystal surfaces. *Surf. Sci.* **1983**, *129*, 59−78.

(19) Gartland, P. O.; Berge, S.; Slagsvold, B. J. Photoelectric work function of a copper single crystal for (100), (110), (111), and (112) faces. *Phys. Rev. Lett.* **1972**, *28*, 738−739.

(20) Tsirkin, S. S.; Eremeev, S. V.; Chulkov, E. V. Inelastic electron-electron scattering for surface states on Cu(110) and Ag(110). *Phys. Rev. B: Condens. Matter Mater. Phys.* **2011**, *84*, 115451.

(21) Jiang, J.; Tsirkin, S. S.; Shimada, K.; Iwasawa, H.; Arita, M.; Anzai, H.; Namatame, H.; Taniguchi, M.; Sklyadneva, I. Yu.; Heid, R.; Bohnen, K.-P.; Echenique, P. M.; Chulkov, E. V. Many-body interactions and Rashba splitting of the surface state on Cu(110). *Phys. Rev. B: Condens. Matter Mater. Phys.* **2014**, *89*, 085404.

(22) Straube, P.; Pforte, F.; Michalke, T.; Berge, K.; Gerlach, A.; Goldmann, A. Photoemission study of the surface state at $\bar{Y}$ on Cu(110): Band structure, electron dynamics, and surface optical properties. *Phys. Rev. B: Condens. Matter Mater. Phys.* **2000**, *61*, 14072.

(23) Plummer, E. W.; Shi, J.; Tang, S.-J.; Rotenberg, E.; Kevan, S. D. Enhanced electron-phonon coupling at metal surfaces. *Prog. Surf. Sci.* **2003**, *74*, 251−268.

(24) Zhang, G. Ph.D. Dissertation, University of Göttingen, 1990; Max-Planck-Institut für Strömungsforschung, Report No. 102 (1991).

(25) Michaelson, H. B. Work function of elements and its periodicity. *J. Appl. Phys.* **1977**, *48*, 4729−4733.

(26) Hinch, B. J.; Koziol, C.; Toennies, J. P.; Zhang, G. Evidence for quantum size effects observed by helium atom scattering during the growth of Pb on Cu(111). *Europhys. Lett.* **1989**, *10*, 341−346.

(27) Speight, J. In *Lange's Handbook of Chemistry*, 16th ed.; McGraw Hill: New York, 2005, Vol. *1*, p 132.

(28) Sugawara, K.; Sato, T.; Souma, S.; Takahashi, T.; Arai, M.; Sasaki, T. Anisotropic spin-orbit interaction in Sb(111) surface studied by high-resolution angle-resolved photoemission spectroscopy. *J. Magn. Magn. Mater.* **2007**, *310*, 2177−2179.

(29) Campi, D.; Bernasconi, M.; Benedek, G. Phonons and electron-phonon interaction at the Sb(111) surface. *Phys. Rev. B: Condens. Matter Mater. Phys.* **2012**, *86*, 075446.

(30) Ernst, H.-J.; Hulpke, E.; Toennies, J. P. Helium-atom-scattering study of the structure and phonon dynamics of the W(001) surface between 200-K and 1900-K. *Phys. Rev. B: Condens. Matter Mater. Phys.* **1992**, *46*, 16081−16105.

(31) Wimmer, E.; Freeman, A. J.; Weinert, M.; Krakauer, H.; Hiskes, J. R.; Karo, A. M. Cesiation of W(001) - work function lowering by multiple dipole formation. *Phys. Rev. Lett.* **1982**, *48*, 1128−1131.

(32) Smith, K. E.; Elliott, G. S.; Kevan, S. D. Reconstruction and fermi-surface of W(001). *Phys. Rev. B: Condens. Matter Mater. Phys.* **1990**, *42*, 5385−5387.

(33) Poole, C. P., Jr.; Zasadinsky, J. F.; Zasadinsky, R. K.; Allen, P. B. Electron-Phonon Coupling Constants. In *Handbook of Superconductivity*, Poole, C. P., Jr., Ed.; Academic Press: New York, 1999; Ch. 9, Sec. G, pp 478−483.

(34) Zhang, Y.-F.; Jia, J.-F.; Han, T.-Z.; Tang, Z.; Shen, Q.-T.; Guo, Y.; Qiu, Z. Q.; Xue, Q.-K. Band structure and oscillatory electron-phonon coupling of Pb thin films determined by atomic-layer-resolved

DOI: 10.1021/acs.jpclett.6b00139
J. Phys. Chem. Lett. 2016, 7, 1016−1021

quantum-well states. *Phys. Rev. Lett.* **2005**, *95*, 096802. Note: This reference reports values of λ that range from 0.7 to 0.9 for 15 to 21 monolayers, respectively, of Pb(111) on a Si(111)-7 × 7 substrate.

(35) Ortigoza, M. A.; Sklyadneva, I. Y.; Heid, R.; Chulkov, E. V.; Rahman, T. S.; Bohnen, K.-P.; Echenique, P. M. Ab initio lattice dynamics and electron-phonon coupling of Bi(111). *Phys. Rev. B: Condens. Matter Mater. Phys.* **2014**, *90*, 195438.

(36) Weitzel, B.; Micklitz, H. Superconductivity in granular systems built from well-defined rhombohedral Bi clusters: evidence for Bi-surface superconductivity. *Phys. Rev. Lett.* **1991**, *66*, 385−388.

DOI: 10.1021/acs.jpclett.6b00139
J. Phys. Chem. Lett. 2016, 7, 1016−1021